ECS Transactions, 35 (6) 83-89 (2011)
10.1149/1.3570849 ©The Electrochemical Society

Microstructure Characterization of Cu-Alloyed GaN Grown by Plasma Assisted Molecular Beam Epitaxy

Teng-Hsing Huang[1], Philipp R. Ganz[2], Liuwen Chang[1*], Daniel M. Schaadt[2] and Jhong-Sing Bao[3]

[1]Department of Materials and Optoelectronic Science/Center for Nanoscience and Nanotechnology, National Sun Yat-Sen University, Kaohsiung 80424, Taiwan, R. O. C.
[2]Institut für Angewandte Physik/DFG-Center for Functional Nanostructures, Karlsruhe Institute of Technology (KIT), 76131 Karlsruhe, Germany

[3]E. B. Tech Co., Ltd./TEMA Tech Co., Ltd., Tainan County 71072, Taiwan, R. O. C.

Cu-alloyed GaN epilayers were prepared by plasma assisted molecular beam epitaxy with Cu-to-Ga beam equivalent pressure ratios of 1.2 to 4.8 %. Islands enriched with Cu are found on the GaN epitaxial layers grown in a Ga-rich environment. The islands are composed of a Cu_9Ga_4 intermetallic phase and GaN with the orientation relationship: $[111]_{Cu9Ga4}//[1\ \bar{2}\ 10]_{GaN}$ and $(10\bar{1})_{Cu9Ga4}//(0001)_{GaN}$. X-ray spectroscopy analyses indicated that the 1.2 % and 4.8 % samples contains 0.10 ± 0.02 wt.%Cu and 0.04 ± 0.03 wt.%Cu, respectively.

Introduction

Dilute magnetic semiconductors (DMS) based on III-nitrides alloyed with transition metal elements have attracted attention recently for possible applications in spintronic devices (1-4). Cu is one of the elements considered for alloying in DMS since first principle calculation predicted that Cu has a ferromagnetic ground state in GaN with a magnetic moment of $2\mu_B$/Cu (5-8). Applying Cu alloying can also avoid controversy regarding the origin of ferromagnetic ordering since metallic Cu and all possible Cu-Ga alloys are not ferromagnetic (3, 4).

Ganz et al. demonstrated very recently that Cu-alloyed GaN epilayers grown by molecular beam epitaxy (MBE) are ferromagnetic at room temperature (9). However, the nominal magnetic saturation is lower than the theoretical prediction using the Cu-to-Ga beam equivalent pressure ratio to determine the nominal Cu doping. This was attributed to the presence of large amount of islands enriched with Cu on the epilayers. Two important issues are raised. First, the formation mechanism of the islands has to be clarified in order to find a proper strategy to improve the Cu incorporation in GaN. Second, the real composition of Cu in GaN has to be determined to justify the magnetic moment contributed by Cu atoms.

The unsolved issues mentioned above provide motivation to study the microstructural characteristics of the islands formed on the Cu-alloyed GaN prepared by plasma assisted MBE. An attempt of analyzing the content of soluble Cu in GaN is also made.

Experimental Methods

Cu-alloyed GaN epilayers were grown on (0001) sapphire substrates by plasma assisted MBE in a Riber compact 21 system equipped with solid-source effusion cells for Ga, Al and Cu. The substrates were glued on Si (001) wafers with In. After outgasing the substrate in a loadlock chamber, the samples were first exposed to an activated nitrogen flux with a pressure of 3.2×10^{-3} Pa at a temperature of 200°C for nitridation of the sapphire surface. After nitridation, an AlN buffer layer of 25 nm thick was deposited under slightly Al-rich condition. Subsequently, Cu-alloyed GaN epitaxial layer was grown at a substrate temperature of 750°C for two hours. The growth rate was estimated to be 65 nm/hour. Three samples having Cu-to-Ga beam equivalent pressure (BEP) ratios of 1.2 %, 2.8 % and 4.8 %, respectively, were prepared in a Ga-rich environment for analysis.

Following the MBE growth, a field emission scanning electron microscope (SEM, JEOL 6330, operating at 5 kV) was used to examine the surface morphology. A detailed microstructure characterization of the epilayers and the islands was carried out by transmission electron microscopy (TEM, FEI Tecnai G2 at 200kV). The cross-sectional TEM samples were either prepared by focus ion beam (FIB, SMI 3050) or by grinding and polishing to ~20 μm thickness followed by Ar ion milling (Gatan PIPS-691) to electron transparency. The Cu content was analyzed by energy dispersive X-ray spectroscopy (EDS) in TEM and by wavelength dispersive X-ray spectroscopy (WDS) in a JEOL JXA-8900R machine at 15 kV.

Results

Figures 1a-c show secondary electron images of the Cu-alloyed GaN having the Cu-to-Ga BEP ratios of 1.2 %, 2.8 %, and 4.8 %, respectively. Numerous islands with sizes of 0.1~20 μm are observed on the flat epilayers. For a low BEP ratio of 1.2% (Fig. 1a), three island morphologies are observed: large, equiaxed islands of 2~10 μm in diameter, long, dendritic ones of ~1 μm wide as well as fine, equiaxed ones of 0.1~1 μm in diameter. For simplicity, these islands are named type-A, -B and -C islands, respectively. By increasing the BEP ratio to 2.8 %, the size of the type-A islands increases (see Fig. 1b). Some of the type-A islands possess a long tail which is similar in shape to the type-B islands. The long tail of the type-A island is therefore named type-A/B island. In Fig. 1c, the number fraction of the type-A islands increases associated with dramatic decreases of that of the type-B and type-C ones. The sample having a BEP ratio of 2.8 % was used for further microstructural analysis since all types of the islands can be easily allocated on the sample.

Cross section TEM samples were prepared by focus ion beam technique to collect morphologic, crystallographic and compositional information of the islands. Figure 2a is a bright field image of a FIB sample made from the center of a type-A island. The image shows that the GaN epilayer is about 100 nm thick whereas the island is as thick as ~400 nm. The island is mainly composed of two parts: a thick top layer with uneven thickness and a bottom GaN layer having a thickness twice as much as that of the neighboring GaN. The interface of the two layers is flat. The top layer contains 68.8 wt.% Cu and 31.2 wt.% Ga according to the energy dispersive X-ray spectrum in Fig. 2b which corresponds

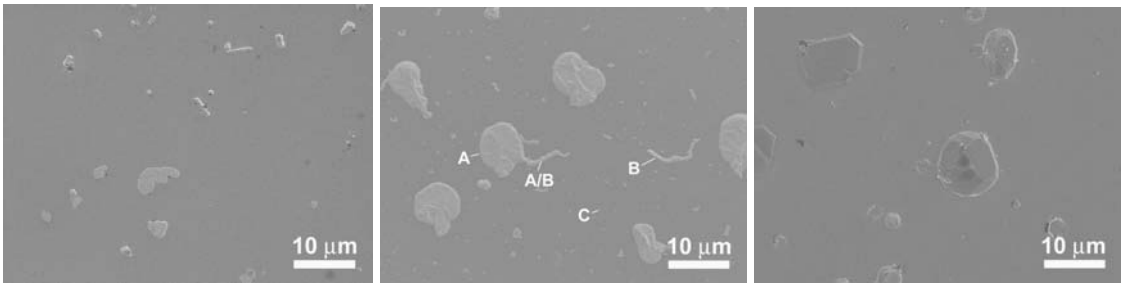

(a) (b) (c)

Figure 1. Secondary electron images of the Cu-alloyed GaN having the Cu-to-Ga BEP ratios of (a) 1.2 %, (b) 2.8 %, and (c) 4.8 %.

to a Cu_9Ga_4 phase. A series of select area diffraction (SAD) patterns were taken from the top layer and two of them are shown in Figs. 2 c-d as examples, confirming that it is a Cu_9Ga_4 intermetallic phase having a cubic unit cell (a=0.8747 nm, $P\bar{4}3m$) (10). The Cu_9Ga_4 layer is a single crystal and indeed possesses a well-defined orientation relationship with the bottom GaN layer. Fig. 2e shows diffraction patterns of Cu_9Ga_4, GaN and AlN taken along the $[10\bar{1}0]$ direction of sapphire. It indicates that both GaN

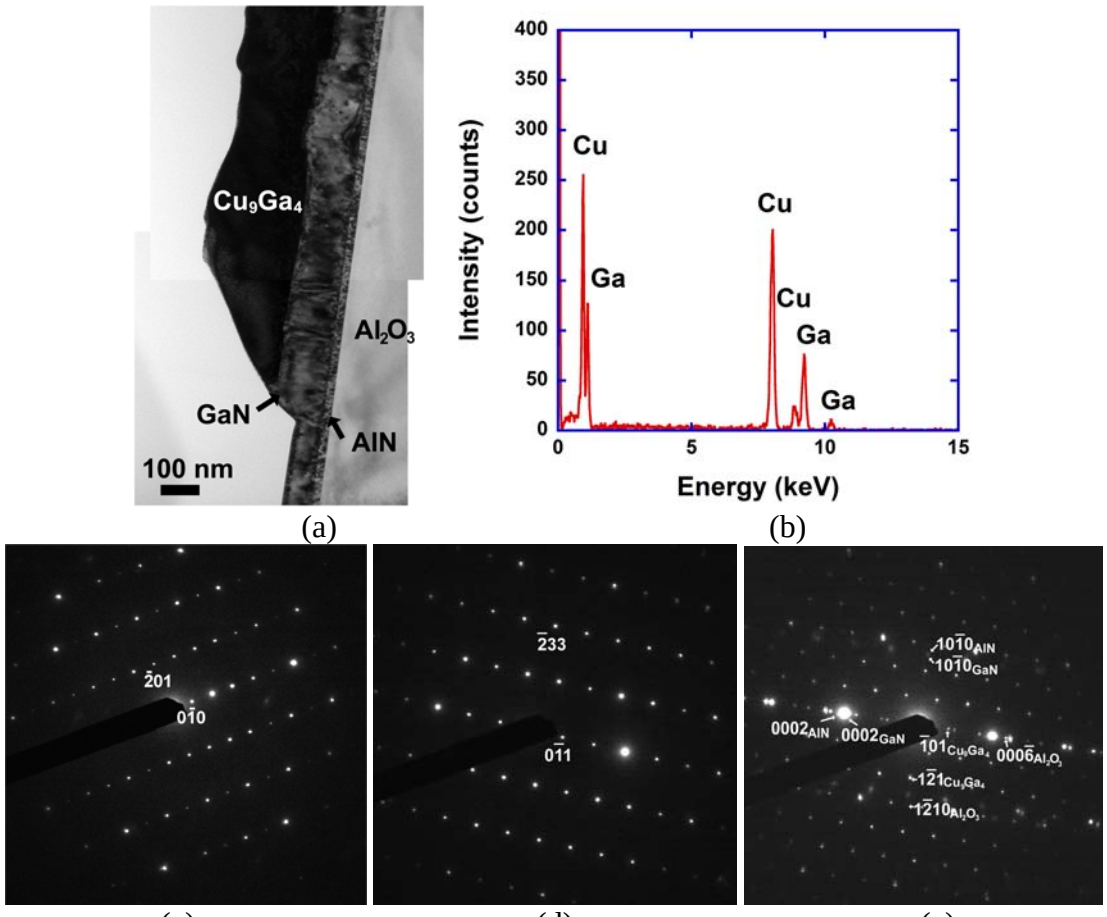

(a) (b)

(c) (d) (e)

Figure 2. (a) Cross-section TEM bright field image of a type-A island. (b) Energy dispersive X-ray spectrum, (c) SAD pattern in [102] zone axis and (d) SAD pattern in [311] zone axis acquired from the top layer of the island. (e) SAD patterns in $[111]_{Cu9Ga4}//[10\bar{1}0]_{sapphire}//[1\bar{2}10]_{GaN}$.

and AlN have their $[1\ \bar{2}\ 10]$ direction parallel to $[10\ \bar{1}\ 0]_{sapphire}$. The orientation relationship between GaN and Cu_9Ga_4 is identified as: $[111]_{Cu9Ga4}//[1\ \bar{2}\ 10]_{GaN}$ and $(10\ \bar{1})_{Cu9Ga4}//(0001)_{GaN}$. In addition, discrete GaN islands scattered on the Cu_9Ga_4 layer are observed.

Figures 3a-c are TEM bright field images of type-A/B, type-B and type-C islands, respectively. Figure 3a shows a type-A/B island of about 2 μm in width. A thick Cu_9Ga_4 crystal is embedded between a thin, flat bottom GaN layer of ~60 nm thick and an irregular top GaN layer. Diffraction analysis (result not shown) indicates that the Cu_9Ga_4 crystal follows the same orientation relationship with the bottom GaN as that described previously. Figure 3b shows the cross section image of a type-B island. The Cu_9Ga_4 phase, having a mountain-like cross section, is also capped by a top GaN layer. The GaN underneath the Cu_9Ga_4 phase is only 10 nm thick. The maze-like pattern shown in the Cu_9Ga_4 phase is probably due to the antiphase domains. However, further studies are needed to clarify this. Figure 3c shows the bright field image of a type-C island of about 500 nm in size. The Cu_9Ga_4 crystal is embedded deeply in GaN. In fact, the Cu_9Ga_4 crystal is grown directly on the AlN buffer layer. Moreover, the type-C island is much thinner than the other types of islands.

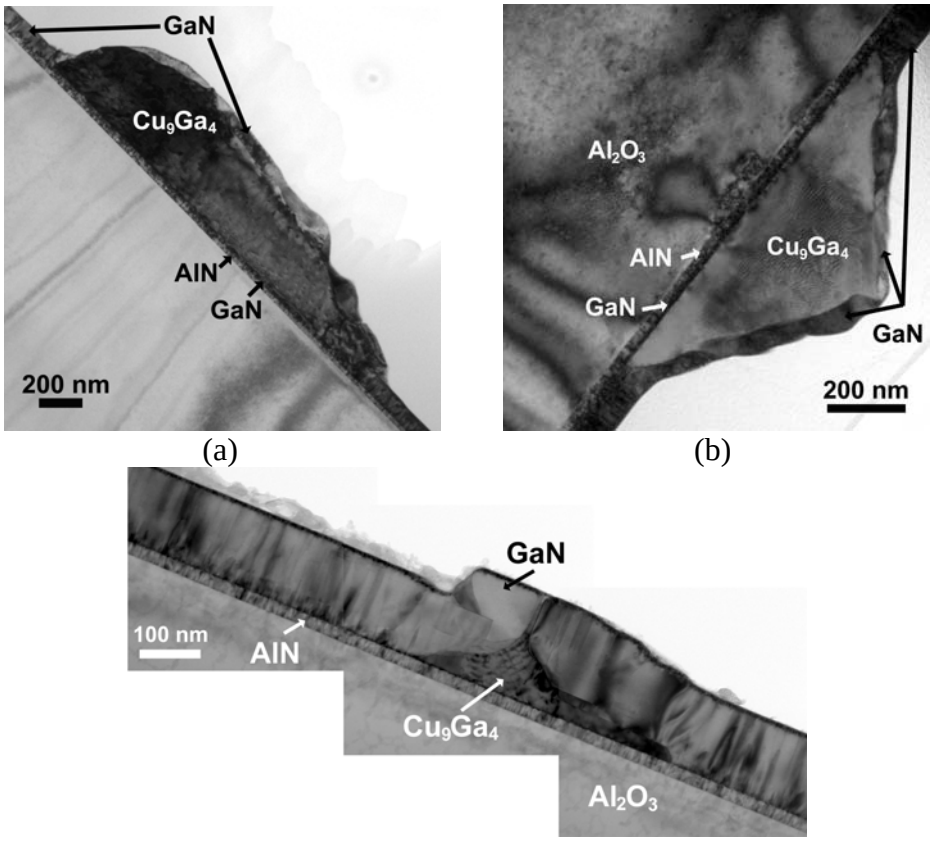

Figure 3. TEM bright field images of (a) type-A/B, (b) type-B, and (c) type-C islands.

Our TEM results reveal that the islands possess basically two kinds of mircostructures. One is composed of three layers: a discrete top GaN, a thick, uneven Cu_9Ga_4 in the middle and a thick, uniform GaN at the bottom. The interface between the Cu_9Ga_4 phase and the bottom GaN is flat and the orientation relationship between them is

identified. This is the microstructure found for type-A islands. Another one is composed of a mountain-like Cu_9Ga_4 crystal capped by a continuous layer of GaN. The smaller the Cu_9Ga_4 phase islands, the thicker the top GaN is. Type-A/B, -B and -C islands all possess the microstructural characteristics. Accordingly, the type-A islands and the type- A/B, -B and -C islands are probably formed from different mechanisms.

Figure 4a is a cross-section TEM image showing a portion of a type-A island. A series of EDS spectra was collected in a scanning transmission mode using an electron beam of 1 nm in diameter and an interval of 5 nm. Figure 4b shows the line scan results of Cu, Ga, N and Al along the dash line marked in Fig. 4a. At the first glance, the Cu content in GaN is higher than that in AlN. However, no Cu Kα peak is found in the EDS spectra acquired from GaN, and the higher Cu intensity probably results from a relatively high fluorescence background. The Cu content in GaN, if any, is accordingly lower than the detection limit of energy dispersive spectroscopy of ~0.1 wt.%.

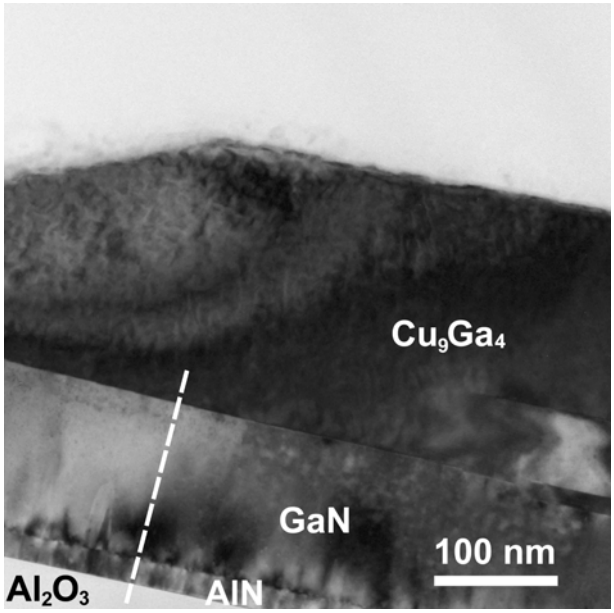

(a)

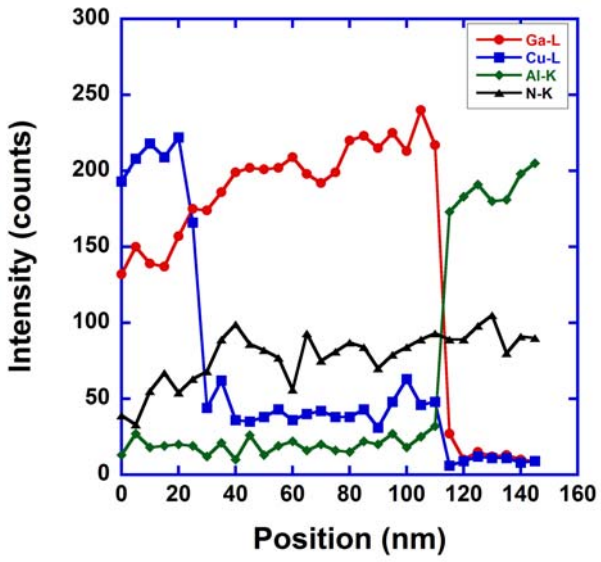

(b)

Figure 4. (a) Cross-section TEM image showing a portion of a type-A island and (b) EDS line scan of Cu, Ga, N and Al along the dash line marked in (a)

In addition, the samples were examined by WDS in in-plane direction. The energy of the electron beam was 15 keV and the excitation volume of the sample was about 1 μm in diameter. Three spots were chosen on the flat GaN epilayer for each sample with the closest island located at least 3 μm away from the center of the spot. The samples were etched by HNO_3 for 5 minutes prior to microanalysis to dissolve all Cu and Cu_9Ga_4 on the surface. Table 1 summarizes the intensities of the Cu and Ga peaks and the corresponding Cu-to-Ga peak ratios of the two samples. The 1.2 % and 4.8 % samples contain 0.10 ± 0.02 wt.% Cu and 0.04 ± 0.03 wt.% Cu, respectively. The Cu content is estimated directly from the Cu-to-Ga peak ratio. It is well known that the generated and measured x-rays in electron beam microanalysis are affected by matrix factors such as atomic number of element (Z), mass absorption of x-ray (A) and x-ray fluorescence (F). A ZAF correction has therefore to be carried out in order to obtain compositions as close to the real values as possible (11). However, the correction has not been performed in the present case since the size of the excitation volume (~1 μm) is larger than the film thickness (~150 nm). ZAF correction is too complicate to be conducted for such a heterostructure (11). It is worth noticing, however, that Cu possesses a high mass absorption coefficient of 271.2 cm^2/g for Ga Kα. This indicates that part of the generated Ga Kα x-ray is absorbed by Cu atoms in GaN and excess Cu Kα radiation can thus be excited by the Ga Kα one. The Cu content given above is probably overestimated.

TABLE 1 Summary of the WDS analyses

Ga-to-Cu BEP ratio, %	Cu Kα, cps	Ga Kα, cps	Cu content, wt.%
1.2	76+/-15	37266+/-761	0.10+/-0.02
4.8	30+/-19	36775+/-198	0.04+/-0.03

The magnetic behavior of the samples coincides well with the compositional analysis. The magnetic moment of dissolved Cu atoms is estimated as 3.4 μ_{sat} /Cu and 2.4 μ_{sat} /Cu, respectively, for the 1.2 % and 4.8 % samples. The values coincide with the theoretical one predicted by Wu et al. within the order of magnitude (5). However, as discussed above, the Cu contents are slightly overestimated and the magnetic moment of Cu atoms derived in the present study is about 50 % higher than that predicted.

Conclusion

Cu-alloyed GaN epilayers were prepared by plasma assisted molecular beam epitaxy in a Ga-rich environment with Cu-to-Ga beam equivalent pressure ratios of 1.2 to 4.8 %. Islands enriched with Cu were found on all the GaN epitaxial layers. The large, equaxed islands are composed of a top Cu_9Ga_4 intermetallic layer and a bottom GaN layer which is about twice as thick as the GaN layer grown from the gas phase. An orientation relationship between GaN and Cu_9Ga_4 was identified as $[111]_{Cu9Ga4}//[1\bar{2}10]_{GaN}$ and $(10\bar{1})_{Cu9Ga4}//(0001)_{GaN}$. The long, dendritic islands and the fine, equiaxed islands are resulted from a different mechanism. Wavelength dispersive X-ray spectroscopy analyses indicated that the 1.2 % and 4.8 % samples contains 0.10 ± 0.02 wt.%Cu and 0.04 ± 0.03 wt.%Cu, respectively.

Acknowledgments

The NSYSU team acknowledges financial support by the National Science Council, R.O.C. under grant number NSC98-2221-E-110-039-MY2, and by the Center for

Nanoscience and Nanotechnology, National Sun Yat-Sen University. The Karlsruhe team acknowledges financial support by DFG and the State of Baden-Württemberg through the DFG-Center for Functional Nanostructures (CFN) within subproject A2.7.

References

1. M. L. Reed, N. A. El-Masry, H. H. Stademaier, M. K. Ritums, M. J. Reed, C. A. Parker, J. C. Roberts, and S. M. Bedair, *Appl. Phys. Lett.*, **79**, 3473 (2001).
2. L. Kronik, M. Jain, and J. R. Chelikowsky, *Phys. Rev. B.*, **66**, 041203-1 (2002).
3. X.Y. Cui, J. E. Medvedeva, B. Delley, A. J. Freeman, N. Newman, and C. Stampfl, *Phys. Rev. Lett.*, **95,** 256404-1 (2005).
4. S. Dhar, L. Pérez, O. Brandt, A. Trampert, K. H. Ploog, J. Keller, and B. Beschoten, *Phys. Rev. B*, **72**, 245203-1 (2005).
5. R. Q. Wu, G. W. Peng, L. Liu, Y. P. Feng, Z. G. Huang, and Q. Y. Wu, *Appl. Phys. Lett.*, **89**, 062505-1 (2006).
6. D. B. Buchholz, R. P. H. Chang, J. H. Song, and J. B. Ketterson, *Appl. Phys. Lett.*, **87**, 082504 (2005).
7. B. Seipel, R. Erni, A. Gupta, C. Li, F. J. Owens, K.V. Rao, N.D. Browning, and P. Moeck, *J. Mater. Res.*, **22**, 1396 (2007).
8. H.-K. Seong, J.-Y. Kim, J.-J. Kim, S.-C. Lee, S.-R. Kim, U. Kim, T.-E. Park, and H.-J. Choi, *Nano Lett.*, **7**, 3366 (2007).
9. P. R. Ganz, C. Sürgers, G. Fischer and D. M. Schaadt, *J. Phys.: Conference Series*, **200,** 062006 (2010).
10. R. Stokhuyzen, J. K. Brandon, P. C. Chien and W. B. Pearson, *Acta Cryst.*, **B30**, 2910 (1974).
11. J. I. Goldstein, A. D. Romig Jr., D. A. Newbury, C. E. Lyman, P. Echlin, C. Fiori, D. C. Joy and E. Lifshin, *Scanning Electron Microscopy and X-ray Microanalysis*, p. 127, Plenum Press, Mew York (1992).